AUTHOR QUERY FORM

Dear Author,

Below are the queries associated with your article; please answer all of these queries before sending the proof back to AIP. Author please indicate the correct color processing option from the list below:

1. Author, please confirm Figure number(s) that should appear as color in print. Please know that any associated mandatory fees will apply for figures printed in color.

2. Author, please confirm Figure number(s) that should appear as color online only, there will be no fees applied.

3. Author, your paper currently does not include any color figures for online or print. If color is needed please indicate which figures it should be applied to and whether it is color in print or online.

Location in article	Query / Remark: click on the Q link to navigate to the appropriate spot in the proof. There, insert your comments as a PDF annotation.
AQ1	Please provide the sponsor/publisher name for Refs [4], [9].
AQ2	Please provide the publisher location for Ref [12].
AQ3	Please provide the complete references for Refs [15]–[17], [19], [20], [22], [27]–[29], and [32].
AQ4	It is unclear what is meant by "/[6] 458–460" in Ref [30]. If this is a separate reference, please provide the full reference, make it a separate numerical reference, and renumber all subsequent references. Because the meaning is unknown, it has been deleted.

Thank you for your assistance.

V. Muñoz, G. A. Rohr, A. L. Cavalieri, and A. G. Tomba Martinez

Experimental Procedure for the Mechanical Evaluation of Oxide-Carbon Refractories by Strain Measurement

ABSTRACT: Experimental issues regarding the implementation of a methodology for obtaining strain-stress curves at high temperatures and in a controlled atmosphere of oxide-C refractories are presented. These curves give a detailed description of the material's mechanical behavior that is not attainable using conventional tests. The method to measure the specimen strain by contact extensometry and the system to control the atmosphere by a gas flow are described. As an example, the experimental study of commercial Al_2O_3-MgO-C refractory bricks used in steel ladles at high temperature (1260 °C) in both air and N_2 atmospheres is presented showing the valuable information obtained applying strain-stress measurements.

KEYWORDS: oxide-C refractories, stress-strain curves, high temperature

Introduction

The mechanical properties of oxide-C refractories [1,2] are associated with the inelastic deformation given by the presence of graphite [3]. This behavior allows the brick to accommodate the applied stress by a certain "flow," thus increasing the fracture strain. Besides the fracture strength parameters currently measured [1,4], such as the modulus of rupture (MOR), the compressive strength (CCS) and the hot modulus of rupture (HMOR), the fracture strain represents equally relevant data. The stress-strain curves provide this information [5–9], and they can be obtained in different temperature and atmospheric conditions. However, this relationship is not commonly measured in ceramics because of the complex equipment required to measure specimen deformation directly in high temperature conditions. The mechanical parameters included in the constitutive equations currently required to feed the finite element method (FEM) codes for calculating the structure can also be obtained from these curves [5,10]. The collection of experimental data (even when cost and time-consuming) is needed to identify refractory behavior laws taking account the main causes of the non-linear behavior while being simple enough for application by industrial users [10]. Together with the analysis of the mechanisms of deformation and fracture, stress-strain relationships are useful for improving material design, which is also a computational assisted process.

In the steelmaking industry (the main consumer of refractory materials), steel processing requires high-performance materials able to withstand the severe chemical environments and the thermal and mechanical loading imposed by the action of the steel bath, the slag and the surrounding atmosphere. The oxide-C refractories like MgO-C and Al_2O_3-MgO-C (AMC) bricks have been used successfully in numerous facilities: basic oxygen (BOF) and electric arc (EAF) steelmaking furnaces (for the whole linings or only in parts such as the slag line) and the floor and walls of vessels such as ladles among others. There is extensive literature pertaining to the most critical properties of these materials, particularly their mechanical and thermomechanical properties, gases and slag corrosion, although a significantly greater amount of literature deals with MgO-C refractory materials. Although there are papers that make use of stress-strain curves [6–9,11], their contribution is significantly low. This situation is even more critical with respect to AMC refractory bricks, for which the amount of this sort of data is negligible.

The aim of this paper is to describe some experimental aspects of the methodology for determining stress-strain curves at high temperature and in a controlled atmosphere of oxide-C refractories bricks in view of addressing scientific and technological fundamentals and developing more accurate models of the mechanical behavior. As a practical example, this methodology is applied to obtain information about the mechanical behavior of commercial AMC refractory bricks used in steelmaking vessels.

Methodology for Determining Stress-Strain Curves

The evaluation of refractory materials is usually done under conditions as similar as possible to the in-service conditions which allow the direct transfer of data to the industrial plant. In other cases, the objective is to obtain basic knowledge about the material behavior in conditions which gives clear and beyond doubt information. The mechanical behavior of oxide-C bricks is rather complex and varies

2 JOURNAL OF TESTING AND EVALUATION

in a permanent way with temperature and time; these material are non-linear in nature. Depending on the temperature, this non-linearity is consequence of a progressive degradation by micro-craking and/or sliding and crumbling of graphite flakes in the low-temperature regime; at higher temperature, the contribution of visco-plasticity (due, for instance, the flow of silicate based glasses) increases [10,11]. Stress-strain curves, ideally measure in tension and compression, characterize this complex behavior and give the experimental data required to model the refractory (constitutive equations) and the lining structure [5,10].

The basic equipment for the stress-strain curves measurement implemented in our laboratory includes a universal servo-hydraulic testing machine (Instron 8501) and an electric furnace (SFL-Severn Ltd.). These curves are based on the direct measurement of the dimensional variation of cylindrical testing specimens under compressive load, which is significant at high temperatures. In the case of materials that react with the atmosphere, a system is required that can modify and control this.

Nowadays, there is no international standard for measuring stress-strain curves. In this paper, the implementation of a standardized methodology [12] to obtain these curves under high temperature conditions and controlled atmosphere is described. The selection of the main testing parameters and conditions has been done based on available ASTM and DIN standards for related mechanical testing of refractories as CCS and creep and information from literature. The methodology described here is specified for the case of oxide-C refractories although it can be used to test different materials with some modifications. In particular, the systems for determining the specimen strain and for controlling atmosphere are depicted; other experimental details as have been published elsewhere [13].

The use of compressive loading is the current practice in refractories owing to the complications associated to tensile tests in brittle materials and also, because compressive stress are prevalent in refractory structures. This is especially true in the case of structures builded with oxide-C bricks [9]. However, the compression testing has disadvantages already known [14]: (a) even though the applied stress is compressive, the actual failure is caused by induced tensile stress, (b) the effects of the friction between the end of specimens and compression platens which caused the barreling of the sample, an overestimation of the fracture strength and a diagonal fracture, (c) the propagation of one crack does not lead to total fracture. In virtue of the benefits of compression tests, these drawbacks are generally minimized by a suitable choice of the specimen height to the lateral dimension ratio and, when is possible, lubrication or using of padding materials in the contact between sample ends and platens. In our case, the high temperature avoided the use of lubrication or padding materials and only the geometry of the specimen was selected to reduce friction effects.

A cylindrical specimen was chosen due to its advantages in compression tests in respect to other geometries [14] and the easier sample preparation (e.g., the minimizing of machining that is only required for the flat faces). The dimensions of the cylinder, ≈ 27 mm in diameter and 45–50 mm in height, were selected taking as reference the values recommended in the creep ASTM and DIN standards [15,16] but considering additional criteria. One of them was the representation of the overall microstructure of the refractory material; regarding this issue, we followed the recommendation of ASTM C133-94 [17] which points out that the smallest dimension of the specimen have to be at least 4 times the larger aggregate. Other criterion was the reduction of both, the friction and backling effects; to realize this, a height/diameter ratio higher than 2 has been proposed for cylinders under compressive loads [14]. Finally, restrictions of: (a) the load capacity (50 kN), limited by the ceramic push-rods (mullite/alumina rods, 60 mm in diameter), (b) the size of the furnance camera, and (c) the structure of atmosphere control system (described below), were also considered to define the specimen dimensions.

Deformation Measurement

There are severe limitations to measuring strain directly (dimensional variation of the specimen, from which the strain is calculated) in the mechanical testing of ceramics at high temperature, which is partly the reason why the use of such mechanical tests is limited. The high temperature rules out the use of strain-gauges, a high-precision device commonly used to measure metal deformation, but limited to low temperature conditions.

An alternative for high temperature measurements is the use of an extensometer; which can be classified into mechanical or contact extensometers and optical extensometers. The contact extensometry is based on the use of mechanical extenders (knives) in contact with the specimen that reproduce its dimensional change and transfer the measurement to an external transducer. This technique was selected because it gives more accurate results than those achieved by other commonly used techniques such us differential dilatometry [18]. Furthermore, the extensometer can be coupled to the machine frame without changes in the load bearing system or the furnace. The measurement is performed on the specimen and is not affected by the deformation of the loading system; the use of long extensors allows an accurate measurement of the small dimensional variations in the refractory specimen. Due to the extensometer configuration, it is also possible to isolate it from the heat dissipated by the furnace, ensuring thermal stability and accurate measurements. Even so, the use of a mechanical extensometer has experimental difficulties associated with it that require special attention to guarantee proper measurement. For example, the contact pressure to prevent sliding of the knives on the specimen surface is a key factor in the operation of this device. It is worth noting that the instrument must have the required accuracy and its calibration verified in accordance with international standards before use.

Two types of extensometers for high temperature were available in our laboratory for determining the axial strain of cylindrical specimens: a commercial capacitive extensometer and a scissor extensometer of our own design and construction [12]. The applicability of each instrument in determining the stress-strain curves of oxide-C refractory bricks was analyzed using commercial MgO-C refractory brick materials, using the strain measured with a clip gauge as reference. It was established that for the range of small deformations prevailing in the stress-strain tests of oxide-C refractory bricks, the capacitive extensometer was more suitable due to the high accuracy achieve by this instrument.
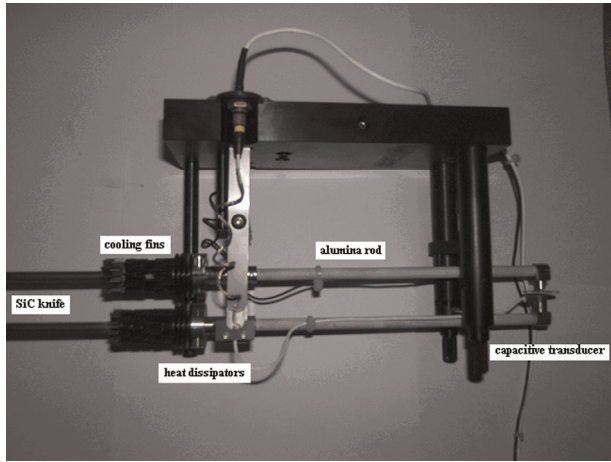
FIG. 1—*Capacitive extensometer (Instron).*

The capacitive extensometer (Fig. 1) is a commercial Instron device. The specifications and instructions of the instrument—mounting, assembly and calibration/verification, positioning on the specimen, and recommendations for optimum performance—are based on the ASTM E83 standard [19]. This instrument consists of two SiC knives which can operate at temperatures up to 1600 °C. The dimensional variation of the specimen causes the extensometer's ceramic knives to move; this is transmitted to the capacitive transducer, which varies the distance between the sensor transducer and reference plate (LVDT). The capacitive transducer is connected to an amplifier-transducer that converts the capacitance into an electrical signal proportional to the dimensional variation of the specimen. According to the specifications manual [20], this extensometer has the characteristics specified in Table 1.

The use of this extensometer requires a prior calibration of the LVDT using a micrometer caliper ($\pm$ 0.001 mm). This extensometer has been calibrated and verified bidirectionally according to ASTM E-83 standard [19] having a maximum strain error of 1×10^{-5} which should be a bidirectional classification A according to the ASTM standard.

Controlled Atmosphere System

Oxide-C refractory materials are very susceptible to reacting with O_2 in the air above 500 °C due to the presence of graphite. The subsequent decarburization modifies its mechanical response by an increase of porosity, a loss of cohesion between the particles and, in consequence, a reduction of the resistant section; other characteristics existing due to the presence of graphite, such as flexibility, also change. Consequently, the presence of the oxidizing agent around the specimen must be reduced in order to minimize the chemical degradation of the refractory specimens during the mechanical testing at high temperature. Several alternative procedures adapted for use with the loading system and the furnace were evaluated, such as the use of a sacrificial material (graphite powder), coating the specimen surface with an alumina-based antioxidant paint and creating a non-oxidizing atmosphere by using a gas flow to replace the air. The first two alternatives were tested and discarded due to practical drawbacks (mainly in the positioning of the extensometer) and their ineffectiveness in avoiding oxidation (especially when using the antioxidant paint).

A system was then designed to generate a practically O_2-free surrounding atmosphere by creating a flow of gas around the testing specimen. For this purpose, a system adapted to the furnace and the loading system (including the extensometer) was designed and built that uses a tube of ceramic material (muffle) inserted into the furnace (Fig. 2) in which a continuous inert gas flow is created. The gas works to remove the oxidant agent (O_2) and reduces its concentration (dilution effect). Under these conditions, the gas flow ensures that overpressure exists inside the muffle that prevents the entry of air at atmospheric pressure. Industrial nitrogen (99.995%) was selected, which represents a compromise between efficiency and cost (in fact, N_2 is not inert with respect to the most common compositions of oxide-C refractory materials). Argon can also be used to generate an inert atmosphere (at higher cost) and also other gases can be used to study their effect on the mechanical behavior of the material.

The muffle must meet the following requirements: (a) it must not interfere in the loading system and allow the actuator to move freely; (b) it must allow for the entry, positioning and free movement of the extensometer, (c) it must not chemically react, deform or break at the testing temperature and atmosphere, and (d) it must not increase the thermal inertia of the furnace excessively. Based on these requirements, a tube of high density alumina (99.9%)

TABLE 1—*Capacitive extensometer specifications.*

Parameter	Value
Accuracy	$\pm$ 0.6 μm[a]
Resolution	0.2 μm
Path	$\pm$ 0.1 mm
Overpath	120% of full scale deflection
Contact force	$\sim$ 35 g[b]
Gauge length	25 mm
Maximum operating temperature	1600 °C

[a]Equivalent to $\pm$ 24 $\mu\epsilon$ in a gauge length of 25 mm.
[b]Adjustable from 0 to 100 g.

FIG. 2—*Front view of the muffle in the furnace chamber.*

4   JOURNAL OF TESTING AND EVALUATION

was selected as the muffle with dimensions consistent with the size of the furnace chamber and the loading system (push-rods of the mullite/alumina rods plus alumina disks $\approx 60\,mm$ in diameter and 10 mm in height). Holes were drilled (diamond drill) on opposite sides of the alumina tube for supplying the gas (alumina tube 10 mm in diameter and 300 mm in length) and the extensometer knives (Fig. 2). Besides minimizing the required flow of N_2, the muffle isolates the heating elements of $MoSi_2$ from this gas, which tends to remove the protective layer of SiO_2 formed in air [21]. A specific study was required in order to calculate the flow of nitrogen needed to reduce decarburization to an acceptable level (≈ 1 wt. %) and which took into account the compromise between the degree of oxidation and the N_2 consumption. As a result, a value of 5 l/min was fixed with a prior period of purging.

The use of this system to control the atmosphere required that some modifications be made to the furnace. These structural changes, together with the cooling effect of the flowing nitrogen, were introduced in a heat transfer model of the system (furnace, load-bearing rods, muffle and specimen) in order to determine the degree to which the furnace's thermal efficiency is reduced [12]. A drop in the maximum temperature from $1600\,°C$ to $1375\,°C$ was estimated, whereas the maximum heating rate changed from 17 to $10\,°C/min$. The maximum temperature reached in the verification tests was $1400\,°C$ and the maximum heating rates were $10\,°C/min$ up to $1100\,°C$ and $5\,°C/min$ up to $1400\,°C$. Other tests were performed to determine the difference between the actual temperature of the tested specimen (using a thermocouple placed into a hole performed in the cylinder) and that of the furnace chamber; it was observed that these differences diminished as the heating advanced and by the end of the heating schedule ($1400\,°C$), the difference was approximately $10\,°C$. Taking into account the compromise between the practical advantages of dispensing with a thermocouple into the specimen (mainly due to volume restrictions) and the error introduced if the temperature of the specimen is taken as being the same as in the furnace chamber (after a suitable stabilization time of 15 min), this last procedure was considered acceptable.

Stress-Strain Tests

This test was performed using the equipment and experimental conditions discussed in the previous sections. They are summarized in an internal protocol [22] which explains in detail how to carry out all the procedures involved, from the switching on of the testing machine to obtaining the stress-strain plot. Basically, the mechanical test consists of the following stages.

(1) Placement of the specimen into the muffle (located in the furnace chamber) and the positioning of the extensometer knives on the specimen surface.
(2) Heating of the specimen (5–$10\,°C/min$, with the gas flow starting at $300\,°C$) up to the testing temperature and stabilization; during this stage, a small compressive load is applied on the specimen to ensure contact with the loading system.
(3) Loading of the specimen into the (actuator) displacement control device until the specimen fractures.
(4) Cooling of the specimen (with gas flowing until $300\,°C$).

The test for obtaining stress-strain curves requires that an increasing monotonic load be applied until specimen failure. This is performed with a displacement control device (of the actuator) since the use of a constant strain rate did not result in stable control of the test. Since the compressive stress develop slowly in most of the application of oxide-C, the measure of the stress-strain behavior have to be done in a similar way if the service condition have to be reproduced [9]. To set the displacement rate, stress-strain curves in the range 0.02 to 0.3 mm/min were obtained on different MgO-C specimens (with pitch and resin binders, in duplicate) to select the appropriate conditions, based on information reported in the literature [11]. The range of suitable strain rates, indicated by a constance of the tangent Young modulus (considering also the experimental error) for small deformations ($< 3 \times 10^{-4}$), was between 6×10^{-5} to 3.3×10^{-4} mm/mm; these values correspond to a displacement rate of 0.1 mm/min. The use of this condition in MgO-C materials gave representative and comparable results. A similar analysis at $1000\,°C$ confirmed that the same rate can be applied in high temperatures tests. The value of 0.1 mm/min may require an adjustment with materials with different properties.

The last stage of cooling is important because chemical changes can still occur in the testing specimens and alter the post-testing analysis essential for the study of the deformation and fracture mechanisms.

In addition to the stress-strain curve, the test provides additional information useful for basic studies of deformation and fracture mechanisms. As part of the process, changes in weight as well as other fracture features, i.e., the number and orientation of cracks, the main crack paths (through the matrix, the interface with the aggregate or aggregates themselves), etc., are evaluated after the mechanical test. When it is possible, other characteristics related to material failure during the test, such as the presence or absence of noise, are evaluated. Mineralogical analysis by X-ray diffraction (XRD), microstructural analysis by optical microscopy, and scanning electron spectroscopy with chemical analysis by energy dispersive X-ray (SEM/EDS) and density and porosity measurement were also performed to study the mechanisms.

Using the stress-strain curves, the mechanical behavior of oxide-C refractory materials (elastic, inelastic, plastic, softening, etc.) is analyzed and mechanical parameters such as elasticity modulus, mechanical strength, fracture strain, and elastic limit are determined. For materials with complex mechanical behavior such as oxide-C refractories, current definitions of the parameters may be inadequate and others have to be used. Depending on the testing methodology used for refractory commercial bricks, maximum errors of $\pm 25\%$ for the elasticity modulus and $\pm 20\%$ for mechanical strength were established.

It is worth noting that the tests can also be performed using loading-unloading cycles that provide additional or complementary information to go with that obtained in increasing monotonic loading tests. In addition to the mechanical behavior of the material, these cyclic tests inform about how much of the deviation from linearity corresponds to a reversible strain and give more accurate values of mechanical properties such as the elastic modulus.

The described methodology may require some variation of the experimental conditions if the material to be studied has

TABLE 2—*Characterization of as-received refractory bricks.*

		AMC1	AMC2
mineralogical composition (XRD; optical microscopy; SEM/EDS)	aggregates	Al_2O_3 (corundum); tabular and brown electrofused	
		-	MgO (periclase); sintered
	matrix	C (graphite): flakes MgO (periclase); sintered Al	
chemical composition (FRX, ICP)	Al_2O_3 (wt.%)	84.0	57.9
	MgO (wt.%)	5.5	27.0
	Fe_2O_3 (wt.%)	1.6	2.0
	Al (wt.%)	1.4	1.4
	others (wt.%)	1.9	3.0
carbon content (TGA)	resin (wt.%)	4.3	5.5
	graphite (wt.%)	1.3	3.2
apparent porosity (DIN EN 993-1 [Ref. 31])	π_a (%)	6.7 ± 0.07	7.8 ± 0.5

characteristics much different from the refractory material used for the adjustment testing (commercial MgO-C bricks).

Stress-Strain Curves of Al_2O_3-MgO-C Refractory Bricks

As example of the application of the depicted methodology to oxide-C refractory materiales, some results and a preliminar discussion are presented for commercial AMC refractory bricks [23–28]; the aim of the analysis is mainly orientated to generate basic knowledge about the material behavior. These are heterogeneous materials made up of a discontinuous phase of alumina and magnesia aggregates submerged in a continuous matrix containing an organic binder (generally a phenolic resin), fine alumina and magnesia grains, graphite flakes, and antioxidant additive particles (metallic or others). Besides their role in inhibiting graphite oxidation, the presence of aluminum or silicon, among others, increases the mechanical performance of these bricks at high temperature through the formation of new phases such as Al_4C_3 (or AlN depending on the N_2/O_2 ratio [29]), which is stable between 700 °C and 1000 °C, and silicon carbide (SiC) and spinel (MgO-Al_2O_3) at higher temperatures [30,31]. This benefit is achieved through factors such as: (a) a decrease in porosity due to the fact that solid products have higher specific volume and/or they crystallize into the pores, and (b) the special morphology of products such as wiskers or skeletal shapes, and/or (c) a binding effect.

Materials

Two types of commercial Al_2O_3-MgO-C bricks used in steelmaking ladle linings were tested and labeled as AMC1 and AMC2. The reported results of the mechanical evaluation are just for one set of specimens. The results of a complete characterization of each material performed by several techniques are summarized in Table 2. In Fig. 3 are shown images of both refractories by optical microscopy. The particles size distribution of tabular alumina aggregates was narrower and the mean size was smaller in AMC1 than in AMC2. Moreover, a larger amount of tabular alumina with respect to electrofused grains was presented in AMC1.

Mechanical Tests

Experimental Conditions—Cylindrical specimens (27 ± 0.1 mm in diameter and 45 ± 1 mm in height) were cut from AMC refractory bricks using a diamond drill (1270 rpm) and a diamond cutting tool (2800 rpm) under optimized conditions. The flats faces of each cylinder were machined with a diamond wheel (70 grit) using a hydraulic oil as coolant/lubricant in order to achieve the required plane-parallelism (0.2 mm). Before the mechanical test, the specimens were dried for 24 h in an oven at 100 °C; the cooling was performed in a desiccator under vacuum.

The experimental conditions for the mechanical testing of AMC refractory bricks were established according to the internal protocol [22] and the requirements of the study. Tests were carried out at 1260 °C in N_2 (flow rate of 5 l/min) using a heating rate of 5 °C/min up to the testing temperature and a constant (actuator) displacement rate of 0.1 mm/min. The dimensional variation in the specimen height was measured with the calibrated capacitive extensometer (gauge length = 25 mm). For comparison, tests at room temperature (RT) and at 1260 °C in air were also performed.
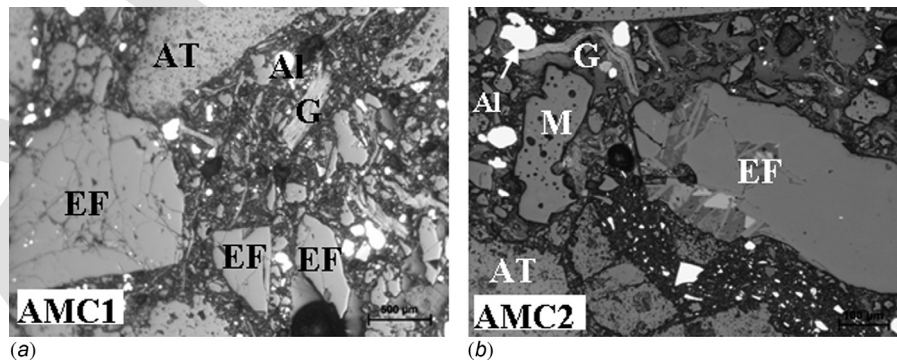

FIG. 3—*Optical microscopy images of as- received AMC refractories (EF: Brown electrofused alumina, AT: Tabular alumina, M: Sintered magnesia, Al: Aluminum, G: Graphite).*
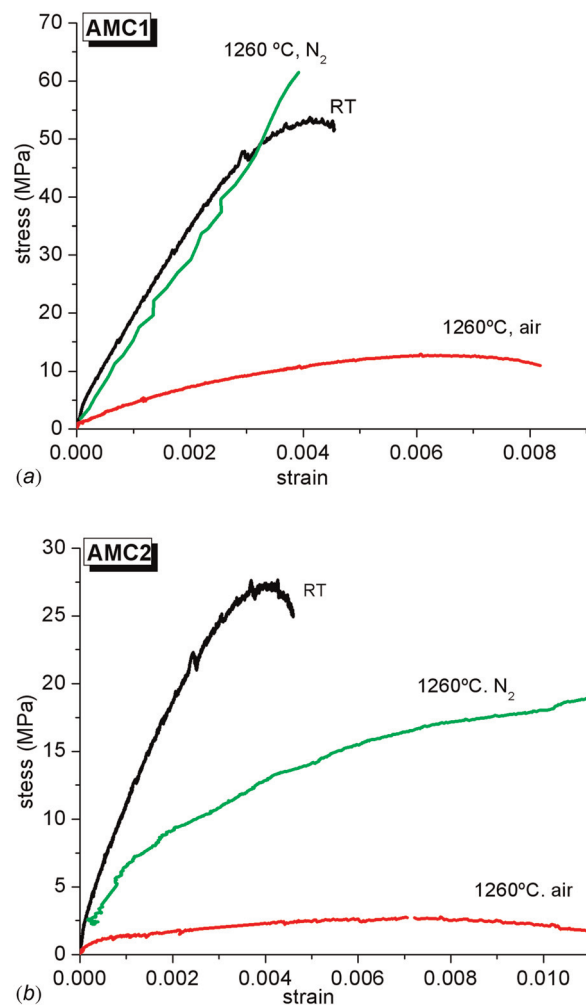
6 JOURNAL OF TESTING AND EVALUATION

(a)

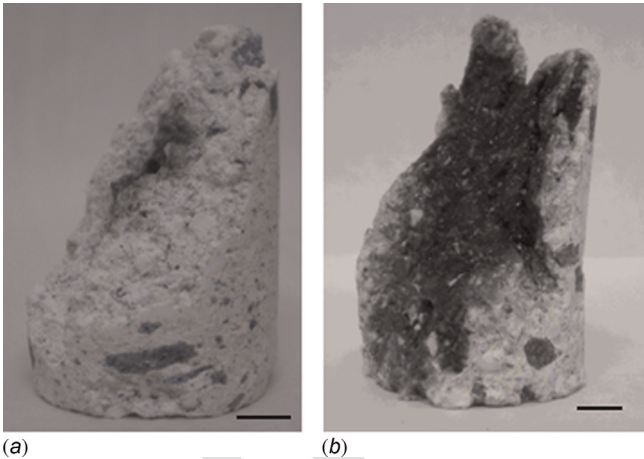FIG. 4—Stress-strain curves of AMC refractories.

(a)   (b)

FIG. 5—AMC1 specimens tested at: (a) 1260°C, air and (b) 1260°C, N_2. Bar: 0.5 cm.

for the as-received materials were employed. In both the refractory 424 materials tested in air and nitrogen, the apparent porosity was higher 425 than the value of the as-received materials due to the increase in the 426 volume of the open pores caused by the transformation of the resin 427 (elimination of volatiles, cracking by volume shrinkage [33]) and 428 graphite oxidation. Other processes such as the reduction in oxide 429 impurities, the spinel and Al_4C_3 formation and the carbothermal 430 reduction of MgO can also be accompanied by the increased 431 appearance of porosity [31]. The variation in open porosity was 432 lower with nitrogen flow than in air, in agreement with the inhibi- 433 tion of resin carbonization [32] and graphite oxidation (Fig. 5) due 434 to a lower oxygen partial pressure. Moreover, the final porosity of 435 AMC2, with its higher initial porosity and larger amounts of graph- 436 ite and resin, was higher than in AMC1 in both atmospheres. 437

The mineralogical analysis of the specimens tested at 1260°C 438 in air and N_2 indicated the formation of spinel in both refractory 439 materials. The spinel DRX peaks were more intense with respect 440 to the other components of the refractory materials in air than in 441 nitrogen for both materials, in agreement with reported data [24]. 442 Carbon as graphite was not identified in the specimens tested in 443 air, which is consistent with the discoloration observed in such 444 testing conditions. No peaks assigned to Al_4C_3 were identified at 445 1260°C in either one of the atmospheres, due to the transforma- 446 tion of this phase into Al_2O_3 below this temperature. The presence 447 of AlN cannot be confirmed because its main diffraction peaks 448 overlap with others present in the as-received refractory bricks 449 and attributed to impurities in the raw materials. However, a dis- 450 tortion of the peaks was observed, especially in AMC1, which 451 could be associated with the formation of this new phase. On the 452 other hand, a significant reduction in the intensity of the peaks 453 assigned to metallic aluminum was observed, indicating that this 454 additive reacted to form spinel, Al_3C_4, Al_2O_3, and/or AlN. 455

Results and Discussion—Stress-strain curves at RT and 411 1260°C (in both air and with the N_2 flow) are plotted in Fig. 4 for 412 AMC2 and AMC1. Images of the AMC1 specimens after mechan- 413 ical testing at 1260°C in air and N_2 are shown in Fig. 5; specimens 414 of AMC2 showed a similar aspect. In both refractory materials 415 tested in air at 1260°C, a discoloration due to the loss of graphite 416 was observed. After the test in nitrogen the discoloration was only 417 superficial showing the effectiveness of the N_2 atmosphere in mini- 418 mizing the graphite oxidative processes. The fracture at room and 419 high temperatures propagated mainly through the carboneous ma- 420 trix and the aggregate/matrix interphases in every specimen. 421

Table 3 shows the post-testing characterization data of speci- 422 mens tested at 1260°C in air and N_2; the same methodologies used 423

At RT, stress-strain curves show a quasi-brittle behavior (devia- 456 tion from linearity) along with a moderate softening (characterized 457 by the gradual diminution of the load-bearing ability as the test 458 progresses), which is more marked in AMC2. The deformation 459 mechanisms causing this non-linearity were mentioned above. The 460 greater porosity and higher content of graphite and resin in AMC2 461 contributed to accentuating this behavior. At 1260°C in air, the 462

TABLE 3—Post-testing characterization (1260°C).

	AMC1		AMC2	
Atmosphere	air	N_2	air	N_2
π_a (%)	23	15	28	18
main phases (XRD)	Al_2O_3, MgO, $MgAl_2O_4$	Al_2O_3, MgO, C, $MgAl_2O_4$	Al_2O_3, MgO, $MgAl_2O_4$	Al_2O_3, MgO, C, $MgAl_2O_4$

quasi-brittle behavior was notably reduced although a little softening persisted; deformation mechanisms similar to those at RT could also have been at work.

In the N_2 atmosphere, AMC2 exhibited a notable non-linear response whereas AMC1 behave in an almost completely linear manner. The behavior of AMC2 was mainly attributed to the incidence of a viscous-plastic mechanism [10,11] owing the higher amount of sintered magnesia with a higher impurities content (such as Fe_2O_3 as hematite, silicates, between others), as shown in Table 2. These impurities form low viscosity phases at $1260\,°C$ (silicate based phases with low melting points [34]) that favor the permanent deformation by viscous flow [10].

The fracture strength (σ_R) and fracture strain (ε_R) were determined from stress-strain curves using the maximum value of stress as the fracture criterion. The Young's modulus was also estimated as the slope of the linear portion of the stress-strain curves. The values of these mechanical parameters are reported in Table 4. At room temperature, the values of the mechanical parameters for both AMC refractory materials were similar to those reported for similar refractory materials [35]. In every tested condition, E and σ_R of AMC1 were higher than those of AMC2 which was mainly attributed to the higher amount of Al_2O_3 (relative to that of MgO) found in AMC1, and the higher mechanical strength and stiffness of the alumina particles, especially those constituting the bonding phase where the fracture propagated (and also considering the intra-aggregate fracture, even as a small contribution). In addition, the higher pore volume and the higher graphite and resin content in AMC2 can help to reduce the value of this mechanical parameter with respect to AMC1.

At $1260\,°C$ in air, the decrease of σ_R and E and the increase of the fracture strain were mainly related to the changes that occurred in the carbonaceous components of the bonding phase (resin and graphite) such as the significant increase in the apparent porosity. In this condition, the negative effects produced by the increase in porosity and the presence of low viscous phases (in AMC2) outbalance the positive effect of the formation of new phases. With respect to the values at RT, the mechanical parameters for AMC2 measured at $1260\,°C$ in N_2 went down. This behavior was attributed to the same factors causing this response in air, but the lower development of the oxidative processes together with the positive contribution of the new phases (namely spinel) led to smaller changes. On the other hand, not only did a recovery of the mechanical properties in N_2 with respect to the test in air at $1260\,°C$ occur in AMC1, the performance also matched that at room temperature. Even the mechanical strength was superior at high temperature. Considering that the porosity determined after the test was significantly higher than that of as-received material—although smaller than the specimen tested at $1260\,°C$ in air—other

processes favoring the structural cohesion, such as the formation of spinel and AlN must have played a dominant role. The sintering of fine particles, the re-crystallization of phases (MgO coming from the reoxidation of $Mg_{(g)}$ produced by carbothermal reduction) and crack closure could also contribute.

The experimental fracture strain was the same for AMC1 and AMC2 at RT whereas at $1260\,°C$, AMC2 exhibited a higher ε_R than AMC1 in air and nitrogen. The difference between ε_R and the strain estimated from σ_R/E ratio correlated with the extent of the non-linear behavior exhibited by the refractory materials. The estimated strain was smaller than the experimental value at RT for both materials. At $1260\,°C$, both values were similar for AMC1 but a significant difference resulted for AMC2 tested at $1260\,°C$ in N_2.

According to these preliminary results, AMC1 seems to have superior mechanical performance at room temperature and $1260\,°C$. However, it is worthy to note that other properties such as the thermal shock resistance and thermal shock damage resistance are benefitted by lower values of Young's modulus and mechanical strength, respectively [36]. In order to clarify the occurrence of the above mentioned processes and the mechanisms operating in AMC2, a SEM/EDX analysis of the specimens tested at high temperature is currently in development and will be the subject of further publications by the authors, along with new mechanical tests at different temperature conditions. Moreover, it is expected that the modeling of the stress-strain curves in a next future steps, gives quantitative data about the contribution of the main mechanisms of non-linear behavior and also, to the structural calculus of the industrial linings where these materials are used.

Conclusions

The main aspects of the design and implementation of a methodology for the mechanical evaluation of oxide-C refractory material were discussed. This methodology is based on the direct measurement of dimensional variations in the tested specimen in order to obtain stress-strain curves in a controlled atmosphere. This test has the advantage of giving much more and complete information about the mechanical behavior than the more commonly used techniques can. Even when some issues are limited by our experience and infrastructure, others have a wide application and serve as guidelines for others who plan to develop this type of complex testing.

As an example, the mechanical evaluation of Al_2O_3-MgO-C commercial refractory bricks using this procedure is also described. From a basic point of view, conventional parameters such as fracture strength and Young's modulus together with others such as the fracture strain were obtained from stress-strain curves; in addition with a preliminary discussion about the mechanical behavior and the mechanisms causing the non-linear response.

TABLE 4—*Mechanical parameters.*

		AMC1			AMC2		
		σ_R (MPa)	ε_R (%)	E (GPa)	σ_R (MPa)	ε_R (%)	E (GPa)
air	*RT*	53	0.4	15.0	27	0.4	9.0
	1260 °C	17	0.8	2.5	11	1.1	1.2
N_2	1260 °C	61	0.4	15.0	19	1.0	4.0

8 JOURNAL OF TESTING AND EVALUATION

References

[1] Alvarez, C., Criado, E., and Baudín, C., "Refractarios de Magnesia-Grafito," *Bol. Soc. Esp. Ceram. Vidrio*, Vol. 31(5), 1992, pp. 397–405.

[2] Ewais, E. M. M., "Carbon Based Refractories," *J. Ceram. Jpn. Soc.*, Vol. 112(10), 2004, pp. 517–532.

[3] Cooper, C. F., "Refractory Application of Carbon," *Brit. Ceram. Trans. J.*, Vol. 84, 1985, pp. 48–53.

[4] Alvarez, C., Criado, E., and Baudín, C., "Hot Modulus of Rupture Automatic Testing Machine," *Proceedings of UNITECR'93*, São Paulo, Brazil, 1993, pp. 435–441.

[5] Schacht, C. A., "Needed Fundamental Thermomechanical Material Properties for Thermomechanical Finite Element Analysis of Refractory Structures," *Fundamentals of Refractory Technology, Ceramic Transactions,* Vol 125, J. Bennett and J. D. Smith, Ed., American Ceramic Society, Westerville, Ohio, 2001, pp. 93–101.

[6] Fitchett, A. M. and Wilshire, B., "Mechanical Properties of Carbon-Bearing Magnesia-I. Resin-Bonded Magnesia and Magnesia-Graphite," *Brit. Ceram. Trans. J.*, Vol. 83, 1984, pp. 54–58.

[7] Fitchett, A. M. and Wilshire, B., "Mechanical Properties of Carbon-Bearing Magnesia-II. Resin-Bonded Magnesia and Magnesia-Graphite," *Brit. Ceram. Trans. J.*, Vol. 83, 1984, pp. 59–62.

[8] Fitchett, A. M. and Wilshire, B., "Mechanical Properties of Carbon-Bearing Magnesia-III. Resin-Bonded Magnesia and Magnesia-Graphite," *Brit. Ceram. Trans. J.*, Vol. 83, 1984, pp. 73–76.

[9] Bell, D. A. and Palin, F. T., "Measurement of High Temperature Mechanical Properties of Refractories Containing Carbon," *Proceedings of UNITECR'89*, Anaheim, CA, 1989, pp. 1219–1124.

[10] Poirier, J., Gasser, A., and Boisse, P., "Thermo-Mechanical Modelling of Steel Ladle Refractactory Structures," *Interceram*, 54(3), 2005, pp. 182–188.

[11] Robin, J. M., Berthaud, Y., Schmitt, N., Poirier, J., and Themines, D., "Thermomechanical Behaviour of Magnesia-Carbon Refractactories," *Brit. Ceram. Trans. J.*, Vol. 97, 1998, pp. 1–10.

[12] Rohr, G. A., "Evaluación Mecánica de Materiales Refractarios con Medidas de Deformación a Alta Temperatura y en Atmósfera Controlada," Undergradute thesis, Materials Engineering. Fac. Ingeniería-UNMdP, 2006.

[13] Muñoz, V., Rohr, G. A., Tomba, A. G. M., and Cavalieri, A. L., "Aspectos Experimentales de la Determinacion de Curvas Esfuerzo-Deformacion a Alta Temperatura y en Atmosfera Controlada: Refractarios Al_2O_3-MgO-C," *Bol. Soc. Esp. Ceram. Vidrio*, Vol. 50(3), 2011, pp. 117–124.

[14] Jayatilaka, A. de S., "Fracture of Engineering Brittle Materials," Applied Science Publishers, London, 1979.

[15] ASTM C 832-00, "Standard Test Methods for Measuring the Thermal Expansion and Creep of Refractories Under Load."

[16] DIN 51053 (EN 993-9), "Method of Testing Dense Shaped Refractory Products. Part 9. Determination of Creep in Compression,"

[17] ASTM C 133-94, "Standard Test Methods for Cold Crushing Strength and Modulus Rupture of Refractories."

[18] Hemrick, J. G., "Creep Measurement and Analysis of Refractories," *Fundamentals of Refractory Technology, Ceramic Transactions*, Vol. 125, J. Bennett and J. D. Smith, Ed., American Ceramic Society, Westerville, Ohio, 2001, pp. 171–193.

[19] ASTM E83-94, "Standard Practice for Verification and Classification of Extensometers."

[20] Manual Instron, "Capacitive Extensometer Specifications," 3118–230/1600 °C.

[21] Chou, T. C. and Nieh, T. G., "Pest Desintegration of Thin $MoSi_2$ Films by Oxidation at 500 °C," *J. Mater. Sci.*, Vol. 29, 1994, pp. 2963–2967.

[22] Manual de Calidad LANAIS 001, Laboratorio de Materiales Estructurales, División Cerámicos, INTEMA.

[23] Williams, P. and Hagni, A., "Mineralogical Studies of Alumina Magnesia Carbon Steel Ladle Refractories," *Proceeding of UNITECR'97*, New Orleans, LA, 1997, pp. 183–192.

[24] Kamiide, M., Yamamoto, S., Yamamoto, K., Nakahara, K., and Kido, N., "Damage of Al_2O_3-MgO-C Brick for Ladle Furnace," *J. Tech. Assoc. Refract. Jpn.*, Vol. 21, 2001, pp. 252–257.

[25] Miglani, S., and Uchno, J. J., "Resin Bonded Alumina-Magnesia-Carbon Brick for Ladles," *Proceeding of UNITECR'97*, New Orleans, LA, 1997, pp. 193–201.

[26] Gupta, A. D. and Vickram, K., "Development of Resin-Bonded Alumina-Magnesia-Carbon Bricks for Steel Ladle Applications," *Interceram*, Vol. 48(5), 1999, pp. 307–310.

[27] Koley, R. K., Rao, A. V., Askar, S., and Srivastava, S. K., "Development and Application of Al_2O_3-MgO-C Refractory for Secondary Refining Ladle," *Proceeding of UNITECR'01*, Cancún, México, 2001.

[28] Nourbakhsh, A. A., Salarian, S., Hejazi, S. M., Shojaiei, S., and Golestani-Fard, F., "Increasing Durability of Ladle Lining Refractories by Utilizing Al_2O_3-MgO-C Bricks," *Proceeding of UNITECR'03*, Osaka, Japan, 2003, pp. 499–502.

[29] Liu, G., Li, H., Yang, B., and Wang, J., "The Influence of the Heat-Treating Atmospheres on Al_2O_3-C Materials with Al Addition," *Proceeding of UNITECR'05*, (Orlando, USA), 2005, pp. 87–91.

[30] Taffin, C. and Poirier, J., "The Behaviour of Metal Additives in MgO-C and Al_2O_3-C Refractories," *Interceram*, Vol. 43(5), 1994, pp. 354–358.

[31] Baudín, C., Alvarez, C., and Moore, R., "Influence of Chemical Reactions in MgO-Graphite Refractories: I, Effect on Texture and High-Temperature Mechanical Properties," *J. Am. Ceram. Soc.*, Vol. 82(12), 1999, pp. 3529–3538.

[32] DIN EN 993-1,1995, "Method of Test for Dense Shaped Refractory Products. Determination of Bulk Density, Apparent Porosity and True Porosity," DIN 51056.

[33] Rand, B., and McEnaney, B., "Carbon Binders From Polymeric Resins and Pitch Part I-Pyrolisis Behaviour and Structure of the Carbons," *Brit. Ceram. Trans. J.*, Vol. 84, 1985, pp. 175–165.

[34] Lee, W. E. and Rainforth, W. M., "Ceramic Microestructures, Property Control by Processing," Chapman and Hall, New York, 1994.

[35] Musante, L., Muñoz, V., Labadie, M. H., and Tomba Martinez, A. G., "High Temperature Mechanical Behavior of Al_2O_3-MgO-C Refractories for Steelmaking Use," *Ceram. Int.*, Vol. 37, 2011, pp. 1473–1483.

[36] Hasselman, D. P. H., "Thermal Stress Resistance of Engineering Ceramics," *Advanced Ceramics II*, S. Sòmiya, Ed., Elsevier, New York, 1988.

AQ1 AQ2 AQ3 AQ4